Journal of Alloys and Compounds 509 (2011) 4386–4389

Contents lists available at ScienceDirect

Journal of Alloys and Compounds

journal homepage: www.elsevier.com/locate/jallcom

Fabrication of Ti–Cu–Ni–Al amorphous alloys by mechanical alloying and mechanical milling

Hiroaki Kishimura*, Hitoshi Matsumoto

National Defense Academy, Department of Materials Science and Engineering, 1-10-20 Hashirimizu, Yokosuka, Kanagawa 239-8686, Japan

ARTICLE INFO

Article history:
Received 4 November 2010
Received in revised form
21 December 2010
Accepted 25 December 2010
Available online 31 December 2010

Keywords:
Titanium alloys
Mechanical alloying
Mechanical milling
Amorphous

ABSTRACT

Ti-based amorphous alloy powders were synthesized by the mechanical alloying (MA) of pure elements and the mechanical milling (MM) of intermetallic compounds. The amorphous alloy powders were examined by X-ray diffraction (XRD), differential scanning calorimetry (DSC), and scanning electron microscopy (SEM). Scanning electron micrographs revealed that the vein morphology of these alloy powders shows deformation during the milling. The energy-dispersive X-ray spectral maps confirm that each constituent is uniformly dispersed, including Fe and Cr. The XRD and DSC results showed that the milling time required for amorphization for the MA of pure elements was longer than that of the MM for intermetallic compounds. The activation energy and crystallization temperature of the MA powder are different from those of the MM powder.

1. Introduction

Ti-based bulk amorphous alloys are of significant scientific and commercial interest because of their high tensile strength, and light weight [1,2]. Ti-based bulk amorphous alloys have been developed in many alloy systems and characterized [1,3–8]. However, because a high critical cooling rate is required for amorphous phase formation in Ti-based amorphous alloys, the maximum size of samples produced by rapid quenching techniques is only on the order of a few millimeters for as-cast Ti-based alloys [1].

For alloys that need extremely high cooling rates to form amorphous phase from liquids, the mechanical alloying (MA) of elemental powder mixtures can be an alternative processing route to produce amorphous phase [9–19]. The product produced by MA is in powder form and is suitable for compaction and densification into various shapes. Using several densification methods, the densification of amorphous powder at temperatures above the glass transition temperature in the supercooled liquid regime has been conducted in many alloys [13,15,20–22]. The amorphization of a material is also realized in mechanical milling (MM), which is the milling of uniform-composition powders such as prealloyed intermetallic compound powders. Amorphization reactions depend on the starting material because of the difference in free energy between those materials [18,19,23]. The dependence of such reactions on the starting material for amorphous formation by a mechanical process has been extensively investigated in some alloy systems. However, comparisons of the amorphization between MA and MM in Ti-based multicomponent alloys are limited.

In this study, amorphous powder alloys were synthesized by MA of pure elemental powders and by MM of prealloyed intermetallic compounds. A comparison of the thermal stability and crystallization behavior of both amorphous powders was conducted.

2. Experimental

MA and MM were conducted with high-energy vibrating ball-mill equipment with a water-cooled jacket (Super Misuni NEV-MA8, Nisshin Giken, Japan) under vacuum [24]. No process control agent was used. The vessel of 120 cm^3 volume and balls were made of stainless steel. The diameter and weight of each ball was 10 mm and 5.7 g, respectively. For the MA experiment, Ti, Cu, Ni, and Al powders of at least 99.9% purity were used. The particle size of starting Ti, Cu, Ni, and Al powder is 300, 100, 300, and 100 mesh, respectively. The nominal composition of the powder mixture was $Ti_{60}Cu_{15}Ni_{15}Al_{10}$. For the MM experiment, a master alloy with the nominal composition $Ti_{60}Cu_{15}Ni_{15}Al_{10}$ (purity >99.9%) was synthesized by arc melting in a titanium-gettered argon atmosphere. The master-alloy ingot was remelted at least 4 times and crushed to crystalline powder. The resulting master-alloy powder, with particles of less than 1 mm in diameter, was used for MM. The ball-to-milled material weight ratio for both experiments was 11:1. Vibration frequency for both experiments was 12 Hz. Small amounts of powder were sampled after selected milling times for structural examination. The structural nature of the samples was examined using X-ray diffraction (XRD; Rint2200, Rigaku, Japan) analysis with Cu Kα radiation. The thermal stability of the samples was investigated by differential scanning calorimetry (DSC; DSC-60, Shimadzu, Japan) at a heating rate of 10–60 K/min. The microstructures of the sample were characterized using a scanning electron microscopy (SEM; SU6600, Hitachi, Japan) system equipped with an energy-dispersive X-ray (EDX) spectrometer (X-max, Oxford Instruments, UK).

* Corresponding author. Tel.: +81 46 841 3810; fax: +81 46 844 5910.
E-mail address: kisimura@nda.ac.jp (H. Kishimura).

0925-8388/$ – see front matter © 2011 Elsevier B.V. All rights reserved.
doi:10.1016/j.jallcom.2010.12.181

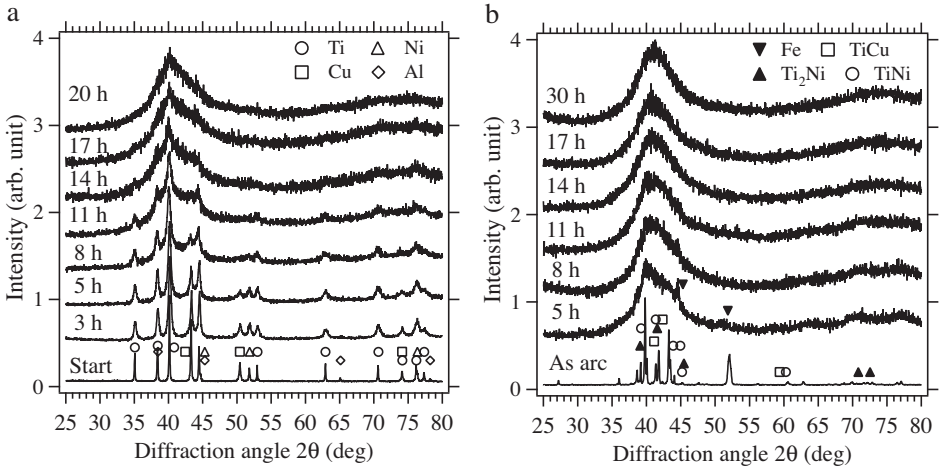

Fig. 1. X-ray diffraction traces of $Ti_{60}Cu_{15}Ni_{15}Al_{10}$ alloy powders after various hours of (a) mechanical alloying and (b) mechanical milling.

3. Results and discussion

Fig. 1 shows the XRD patterns of the MA and MM powders after several hours of milling. The bottom curve shows the XRD patterns of the powder mixture and arc-melted alloy. For the MA powders, only elemental peaks are detected after 5 h of MA (Fig. 1(a)). After 8 h of MA, a broad peak corresponding to an amorphous structure appears at $2\theta = 35–45^\circ$, superimposed on the elemental peaks. A gradual decrease in the intensity of the elemental peaks and an increase in the intensity of the broad peak with increasing MA time are observed. Note that no additional peaks corresponding to intermetallic compounds are observed. After 20 h of MA, the elemental peaks become indistinguishable. For the arc-melted alloy, sharp peaks corresponding to crystals of intermetallic compounds are observed on the XRD pattern. After 5 h of MM, most of the peaks disappear and a broad peak at $2\theta = 35–45^\circ$ arises (Fig. 1(b)). In contrast to the results of the MA powder, no diffraction peaks of any crystalline metallic phases are observed after 11 h of MM. A peak corresponding to Fe also appears on the XRD patterns of MM alloy at $2\theta = 45^\circ$. This indicates that contaminants from milling equipment are mixed during the ball milling.

Fig. 2 shows a comparison of the DSC traces for amorphous powders after several hours of milling at a heating rate of 10 K/min. Both powders show an exothermic crystallization, a peak intensity increase and a peak temperature shift to higher temperatures with increasing time. For the MA powder, the DSC traces show an endothermic reaction characteristic of the glass transition at low temperatures, followed by a sharp exothermic crystallization peak at higher temperatures. However, for the MM powder, the DSC traces show no evident peaks for the glass transition. A small exothermic peak appears in the DSC trace of the 5-h-MM powder, in contrast to that of the 5-h-MA powder. This result is similar to that of the XRD analysis.

The above results indicate that the time required for the transformation into an amorphous structure in MM is much shorter than that in MA for the elemental powders, as expected [19]. For Ni–Ti and Ni–Nb alloys, Schwarz and Koch reported that the required processing times for a fully amorphous product both by MA starting from a mixture of pure-element powders and by MM using crystalline intermetallic compounds are approximately the same [23]. On the other hand, the required processing time for a fully amorphous powder of $Ni_{61}Zr_{39}$ from a crystalline alloy is approximately half the time required by MA using elemental powders [25]. This discrepancy in milling period may result from differences in experimental conditions, contamination, and diffusion characteristics of alloys.

Generally, the temperature for onset of crystallization is strongly associated with the nucleation process, and the peak temperature is related to the growth process [26]. The apparent activation energies of characteristic temperatures can be determined from the peak shifts of the heating DSC curves at different heating rates and using the Kissinger equation [27] and the Ozawa

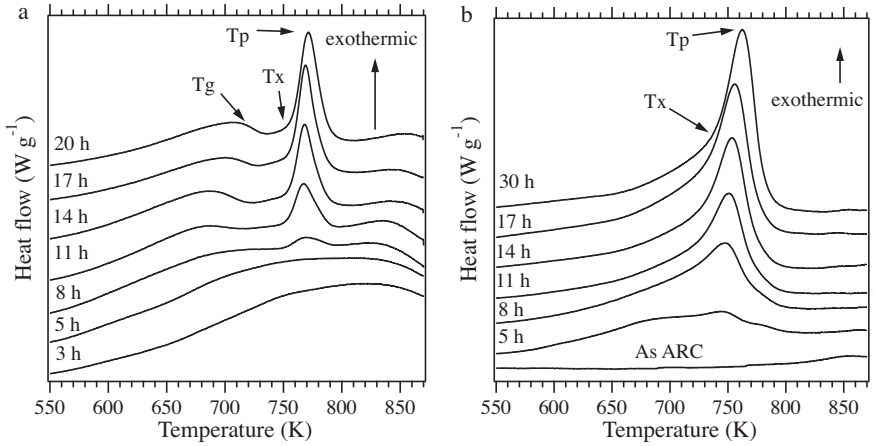

Fig. 2. DSC thermogram determined by heating $Ti_{60}Cu_{15}Ni_{15}Al_{10}$ alloy powders at a rate of 10 K/min of after various hours of (a) mechanical alloying and (b) mechanical milling.

equation [28]. After final milling time, the temperature for onset of crystallization, T_x and the peak temperature, T_p for the MA and MM, and the glass transition temperature, T_g, for the MA are obtained at 10 K/min. These obtained temperatures are used for determination of the apparent activation energy. The linear relationships between $\ln(BT^{-2})$ and T^{-1} (Kissinger) and $\ln B$ and T^{-1} (Ozawa) are shown in Fig. 3, where B is the heating rate, R is the gas constant, T is the temperature, and E is the apparent activation energy deduced from the slope. Table 1 shows a summary of the results. Thermal characteristics of $Ti_{60}Cu_{15}Ni_{15}Al_{10}$ alloy obtained by Nguyen et al. [9] are also presented in Table 1. The activation energies, E_p, and the temperatures of crystal growth for the MA and MM powders are similar. On the other hand, the activation energy of nucleation, E_x, for the MA powder is much lower than that for the MM powder, whereas the temperature of nucleation for the MA powder is higher than that for the MM powder. In the Ni–Zr system, differences in the crystallization temperature and activation energy between amorphous alloys from milled crystalline alloy and those from mechanical alloy have been reported [18]. The crystallization temperatures, T_p, and activation energies of crystallization were similar for melt-spun and ball-milled ribbon. However, these parameters were markedly lower for MA powders from elemental powders [15]. It is indicated that a difference in the type of amorphization reaction can lead to differences in thermal stability and crystallization process.

Fig. 4 shows a SEM image and a composition map of the end product of the MA (Fig. 4a) and MM (Fig. 4b) powders obtained using an EDX spectrometer attached to a SEM system. The surfaces of both the MA and MM powders exhibit the vein morphology typ-

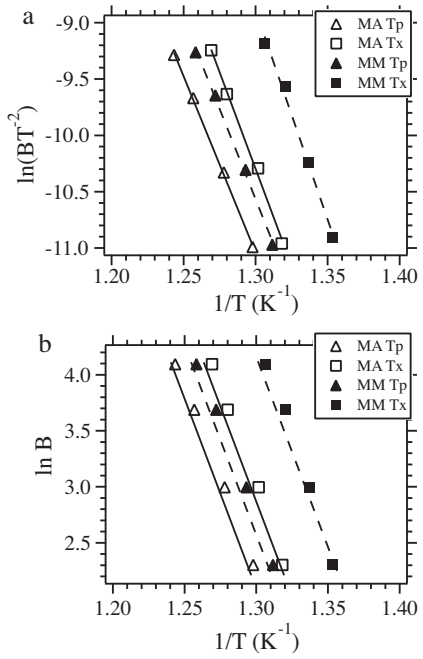

Fig. 3. (a) Kissinger plots of $\ln(BT^{-2})$ versus T^{-1} (b) Ozawa method of $\ln B$ versus T^{-1} obtained from heating DSC scans in both mechanical alloying and mechanical milling samples.

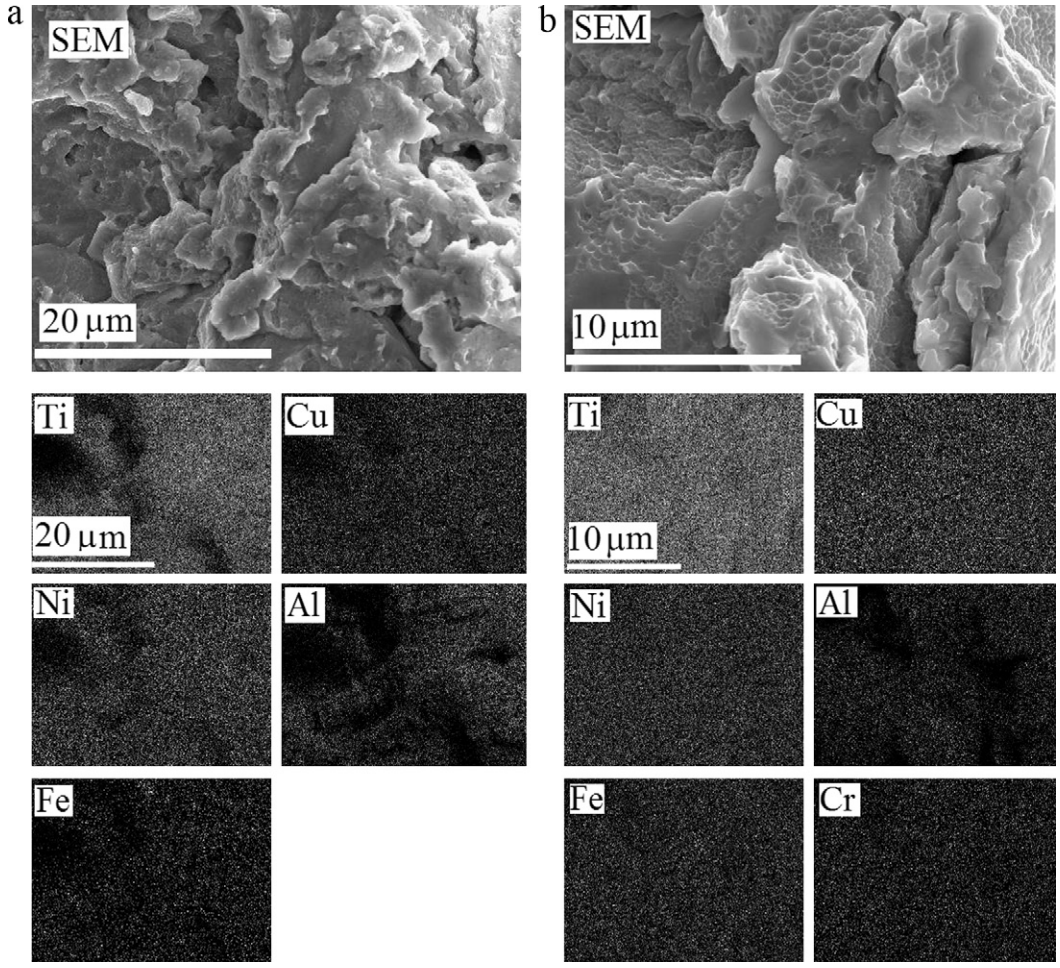

Fig. 4. SEM images and EDX maps showing powders fabricated by (a) mechanical alloying and (b) mechanical milling.

Table 1
Characteristic parameters of crystallization process for $Ti_{60}Cu_{15}Ni_{15}Al_{10}$ alloy powders prepared by MA and MM.

	T_g (K)	T_x (K)	T_p (K)	E_x (kJ/mol) (Kissinger)	E_p (kJ/mol) (Kissinger)	E_x (kJ/mol) (Ozawa)	E_p (kJ/mol) (Ozawa)
MA powder	707	759	770	285.6 ± 12.3	260.5 ± 4.9	298.5 ± 12.2	273.6 ± 4.9
MM powder		739	762	309.2 ± 19.3	266.5 ± 9.3	321.8 ± 19.2	279.4 ± 9.2
Nguyen et al. [9]	678	757	765				

T_x and T_p, and T_g are obtained at 10 K/min.

ically seen in fractographs of metallic glass [8]. It is shown that the distributions of each constituent element are similar and that none of them are localized, confirming the compositional homogeneity of the alloys. In addition, the EDX spectroscopy reveals that the amorphous powders from the MA and MM powders contain Fe and Cr at several atomic percentages. These elements are regarded as contaminants from the vessel and balls during the milling. It is speculated that the difference in thermal characteristic between the present and previous results [9] is attributed to such contaminants accompanied by composition deviation [14].

4. Conclusion

Amorphization processes, and the structural and thermal characteristics of Ti-based amorphous alloys produced by the mechanical alloying of elemental powders and by the mechanical milling of intermetallic compound powder are studied. The XRD patterns and DSC traces show that the processing time required for amorphization by MM is shorter than that by MA. It is found that there are differences in activation energy and temperature of the onset of crystallization between both alloys. It is indicated that a difference in the type of amorphization reaction can lead to differences in thermal stability and crystallization process. Contaminants coming from vessel and balls during the milling are revealed using EDX spectroscopy, and the composition deviation caused by the milling may affect the thermal characteristics and amorphization process of the $Ti_{60}Cu_{15}Ni_{15}Al_{10}$ alloy.

References

[1] T. Zhang, A. Inoue, Mater. Trans. JIM 39 (1998) 1001.
[2] X.H. Lin, W.L. Johnson, J. Appl. Phys. 78 (1995) 6514.
[3] A. Inoue, N. Nishiyama, K. Amiya, T. Zhang, T. Masumoto, Mater. Lett. 19 (1994) 131.
[4] K. Amiya, N. Nishiyama, A. Inoue, T. Masumoto, Mater. Sci. Eng. A 179–180 (1994) 692.
[5] D.E. Polk, A. Calka, B.C. Giessen, Acta Met. 26 (1978) 1097.
[6] D.V. Louzguine, A. Inoue, Scripta Mater. 43 (2000) 371.
[7] J.Z. Chen, S.K. Wu, J. Non-Cryst. Solids 288 (2001) 159.
[8] W. Ma, H. Kou, J. Li, H. Chang, L. Zhou, J. Alloys Compd. 472 (2009) 214.
[9] H. Nguyen, J. Kim, Y. Kwon, J. Kim, J. Mater. Sci. 44 (2009) 2700.
[10] R. Nagarajan, S. Ranganathan, Mater. Sci. Eng. A 179–180 (1994) 168.
[11] K.B. Kim, S. Yi, S.H. Kim, W.T. Kim, D.H. Kim, Mater Sci. Eng. A300 (2001) 148.
[12] I. Jeng, P. Lee, J. Chen, R. Jeng, C. Yeh, C. Lin, Intermetallics 10 (2002) 1271.
[13] P.P. Choi, J.S. Kim, O.T.H. Nguyen, Y.S. Kwon, Mater. Lett. 61 (2007) 4591.
[14] C.K. Lin, S.W. Liu, P.Y. Lee, Metal. Mater. Trans. A 32A (2001) 1777.
[15] D. Oleszak, D. Kolesnikov, T. Kulik, Mater. Sci. Eng. A 449–451 (2007) 1127.
[16] D. Oleszak, L. Wierzbicki, T. Kulik, J. Phys.: Conf. Ser. 144 (2009) 012023.
[17] R.B. Schwarz, Scripta Mater. 34 (1996) 1.
[18] A.W. Weeber, H. Bakker, Phys. B 153 (1988) 93.
[19] C. Suryanarayana, Prog. Mater. Sci. 46 (2001) 1.
[20] P.Y. Lee, W.C. Liu, C.K. Lin, J.C. Huang, Mater. Sci. Eng. A 449–451 (2007) 1095.
[21] P.P. Choi, J.S. Kim, O.T.H. Nguyen, D.H. Kwon, Y.S. Kwon, J.C. Kim, Mater. Sci. Eng. A 449–451 (2007) 1119.
[22] J. Bach, B. Krueger, B. Fultz, Mater. Lett. 11 (1991) 383.
[23] R.B. Schwarz, C.C. Koch, Appl. Phys. Lett. 49 (1986) 146.
[24] C.H. Lee, M. Mori, T. Fukunaga, U. Mizutani, Jpn. J. Appl. Phys. 29 (1990) 540.
[25] A.W. Weeber, H. Bakker, F.R. de Boer, Europhys. Lett. 2 (1986) 445.
[26] W.K. An, X. Xiong, Y. Liu, J.H. Li, A.H. Cai, Y. Luo, T.L. Li, X.S. Li, J. Alloys Compd. 486 (2009) 288.
[27] H.E. Kissinger, Anal. Chem. 29 (1957) 1702.
[28] H.R. Wang, Y.L. Gao, Y.F. Ye, G.H. Min, Y. Chen, X.Y. Teng, J. Alloys Compd. 353 (2003) 200.